Journal of Crystal Growth 106 (1990) 695–704
North-Holland

PRESSURE-INDUCED NUCLEATION AND GROWTH PROCESSES IN THE DIAMOND ANVIL CELL

M. RIEDEL and R. DÄSSLER

Institute of High Pressure Research, Academy of Sciences of the GDR, DDR-1561 Potsdam, German Dem. Rep.

Received 4 December 1989; manuscript received in final form 18 June 1990

The kinetics of pressure-induced first-order phase transitions in the diamond anvil cell (DAC) is investigated. It is shown, that the transition kinetics is considerably influenced by the pressure depletion in the sample volume during the different stages of transformation, especially at low overpressures above equilibrium. A modified Avrami model including the change of degree of metastability is proposed and is checked by experimental data from the B1 → B2 transition in potassium iodide. As a consequence, the double-logarithmic plot of the transformed volume fraction $\ln(-\ln(1-\xi))$ versus $\ln(t)$ reveals a nonlinear bending, which could lead to some misleading conclusions in the interpretation of the experimental results. The observed modifications should be present in any first-order phase transition with a significant volume jump in the DAC under hydrostatic conditions.

1. Introduction

The kinetics of nucleation and growth processes in dependence of various thermodynamic control parameters has been a subject of considerable interest in the last years. Usually, first-order phase transitions are considered to take place in metastable systems with given energy barriers in dependence of the supersaturation. An important example is the well-known Avrami model [1], which describes the nucleation and growth process in an infinite volume. As a consequence, the thermodynamic parameters temperature and pressure are supposed to remain constant during the transformation. On the other hand, in many experimental situations, the relevant thermodynamic conditions are rather isothermal-isochoric than isothermal-isobaric. Therefore, a noticeable pressure change occurs during the different transformation stages, and the Avrami theory does not apply. In order to describe this phenomenon, the underlying theoretical model must be modified to include the pressure depletion in the sample volume.

Our aim is the investigation of pressure-induced first-order phase transitions in the diamond anvil cell (DAC). Since the sample volume in the DAC is very small (of the order of 10^{-12} m^3), the transition kinetics may be influenced considerably by the pressure depletion, especially in the neighbourhood of the equilibrium line, and it is necessary to correct the experimentally obtained kinetic data. On the other hand, the use of pressure quenches for the study of equilibrium relaxation processes seems to be a favourable method, since the very fast establishment of mechanical equilibrium in the DAC allows for rapid and uniform changes of the thermodynamic conditions.

In the present paper, we use the well-known B1 → B2 transition in potassium iodide KI to demonstrate the influence of the finite system volume on the relaxation kinetics in the DAC. The experimental observations are explained with the help of a modified Avrami theory.

2. Model description

Following the classical development of the theory of the kinetics of first-order phase transitions by Johnson and Mehl [2], Avrami [3–5], and

Kolmogorov [6], the transformed volume fraction ξ of the new phase at time t is given with

$$\xi(t) = 1 - \exp\left[- \int_0^t I^{\mathrm{V}}(s)\ v_s(t)\ \mathrm{d}s \right], \tag{1}$$

where $I^{\mathrm{V}}(s)$ is the homogeneous nucleation rate per unit volume and $v_s(t)$ is the volume of a nucleus grown from time s to t. The derivation of eq. (1) implies a uniformly acting driving force throughout the material and an infinite system volume in the thermodynamic limit. Although the first condition is in a good agreement with our experimental setup, the second condition is violated. Therefore we have to take into account the pressure depletion according to the isochoric boundary condition via a second relation,

$$p(t) = F(t;\ \xi(t)), \tag{2}$$

for a new independent order parameter, the pressure $p(t)$. Fortunately, the establishment of mechanical equilibrium in the sample volume is in most cases much faster than the phase transition kinetics. Then $p(t)$ is "slaved" through $\xi(t)$ [7], and one may substitute the complicated functional dependence F by a simple Taylor expansion of the pressure–volume relation.

As a consequence of eq. (2), the work of formation of a critical nucleus is qualitatively changed. This is shown for an important example, the classical droplet-model, in fig. 1. For isochoric constraints an additional stable state of the grown drop exists in a certain range of the supersaturation, and the phase transition is terminating into this state [8,9]. A quite similar behaviour, the appearance of a new stable state, we have to

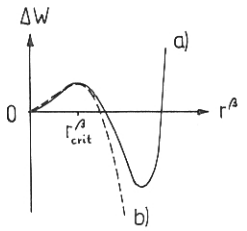

Fig. 1. Qualitative change of the work of formation ΔW of a spherical nucleus with radius r^β for given initial supersaturation in the classical droplet model (after Ulbricht et al. [9]): (a) under isothermal-isochoric boundary conditions; (b) under isothermal-isobaric boundary conditions.

expect in the case of first-order phase transitions in the DAC with a significant volume jump between the two different phases. For a quantitative formulation, we rewrite eqs. (1) and (2) in the form

$$\xi(t) = 1 - \exp\left[- \int_0^t I^{\mathrm{V}}(s;\ p(s)) \times v_s(t;\ p(s))\ \mathrm{d}s \right], \tag{3}$$

and, with respect to our experimental preparation,

$$p(t) = p(0) - (k_T)^{-1} C^{\mathrm{V}}_{\mathrm{KI}} \delta_{\mathrm{vol}}\ \xi(t). \tag{4}$$

Here, $k_T = V^{-1}(\partial V/\partial p)_T$ is the isothermal compressibility of the pressure-transmitting medium, $C^{\mathrm{V}}_{\mathrm{KI}}$ is the volume fraction of the crystals in the gasket hole, and $\delta_{\mathrm{vol}} = \Delta V/V_\alpha$ is the relative volume jump during the phase transformation.

2.1. Nucleation rate

According to the classical Becker–Döring theory, the volume nucleation rate, I^{V}, can be written as [1]:

$$I^{\mathrm{V}} = (K_{\mathrm{V}}/\eta) \exp(-\Delta G^*/kT), \tag{5}$$

where

$$\Delta G^* = 16\pi\sigma^3 V_\alpha^2/3(\Delta\mu)^2,$$

for a spherical nucleus. Here, K_{V} is the kinetic parameter for the volume nucleation, η is the viscosity of the pressure-transmitting medium, ΔG^* is the critical free energy of the nucleus, δ is the interfacial energy between the two phases, V_α is the molar volume of the original phase, and $\Delta\mu$ is the difference of the two chemical potentials. For steady state nucleation, the kinetic parameter, K_{V}, is chosen to be constant. The interfacial energy in general is not well known and is chosen to fit the experimental data.

2.2. Growth from the solution

Based on the thermodynamics of irreversible processes, the general equation

$$\frac{\mathrm{d}r^\beta}{\mathrm{d}t} = \frac{D}{kT}\frac{c^\infty}{c^\beta}\frac{\mu_\alpha - \mu_\beta}{l_0}\left(1 - \frac{r^\beta_{\mathrm{crit}}}{r^\beta}\right), \tag{6}$$

describing the growth of a spherical nucleus with radius r^β from a supersaturated solution, may be derived [10]. Here, D is the diffusion constant, kT is the thermal energy, c^∞ and c^β are the equilibrium concentrations of the solution without and with a nucleus, respectively, r^β_{crit} is the critical nucleus size at given p and T of the metastable phase, and

$$l_0 = \begin{cases} d_0 = \text{constant} \\ \text{for interface controlled growth,} \\ r^\beta(t) \\ \text{for diffusion limited growth.} \end{cases}$$

If the long-range transport to the interface is the dominant (slowest) kinetic process, the location of the moving surface r^β is given by the well-known parabolic growth law

$$r^\beta(t) \sim (Dt)^{1/2}, \tag{7}$$

under appropriate boundary conditions. Otherwise, for interface controlled growth, the growth velocity is time-independent and

$$r^\beta(t) = \gamma\, Dt. \tag{8}$$

The prefactor γ may be expanded near the phase equilibrium in

$$\gamma(p) = \gamma_1(p - p_{\text{eq}}) + \ldots, \tag{9}$$

with a suitable constant γ_1. Modifications of the power laws (7) or (8) due to the impingement of different nuclei or other nonlinear effects are beyond the scope of this treatment. Additionally, we neglect in the following the influence of the finite critical nucleus size.

2.3. *Transformed volume fraction*

The volume fraction of the growing new phase follows from eqs. (3), (5) and (6) together with eq. (4). In differential form, eq. (3) reads

$$\frac{1}{1-\xi}\frac{\mathrm{d}\xi}{\mathrm{d}t} = E(t, t) + \int_0^t \frac{\partial}{\partial t} E(t, s)\, \mathrm{d}s, \tag{10}$$

with the abbreviation

$$E(t, s) = I^{\mathrm{V}}(s;\, p(s))\; v_s(t;\, p(s)).$$

Combining eqs. (4), (5), (8) and (9), one finally obtains

$$\frac{\partial}{\partial t} E(t, s) = a_1\big[a_4 - a_3\xi(t)\big]\left(\int_s^t \big[a_4 - a_3\xi(u)\big]\,\mathrm{d}u\right)^2 \times \exp\left(-\frac{a_2}{\big[a_4 - a_3\xi(s)\big]^2}\right),$$

where

$$a_1 = K_{\mathrm{V}}\eta^{-1}\, 4\pi\, \left(c^\infty D p_{\text{eq}} \Delta V / c^\beta d_0 kT\right)^3$$

is the kinetic prefactor,

$$a_2 = \frac{16\pi}{3}\left(\frac{\sigma}{kT}\right)^3\left(\frac{\delta_{\text{vol}}\, p_{\text{eq}}}{kT}\right)^{-2}$$

measures the balance between the interfacial energy σ and the enthalpy jump $\delta_{\text{vol}}\, p_{\text{eq}}$,

$$a_3 = \left(k_T p_{\text{eq}}\right)^{-1} C^{\mathrm{V}}_{\mathrm{KI}}\delta_{\text{vol}}$$

is a constant depending on the experimental preparation, and

$$a_4 = \big[p(0) - p_{\text{eq}}\big]/p_{\text{eq}} = \Delta p/p_{\text{eq}}$$

is the normalized initial overpressure Δp.

3. Experimental

The apparatus consisting of a DAC combined with an image-processing system is described elsewhere [11]. The image-processing system permits a real-time observation of the transformation process in the DAC, as well as continuous image storing and data processing during the phase growth. The principle of the optical determination of the degree of transformation is based on the measurement of the proportion between the two phase areas derived from their differing refractive indices. The measured differences of the brightness are converted into a digitized black-and-white image. which can be analyzed by standard numerical methods. The DAC technique in opposed anvil configuration is a usual method to generate pres-

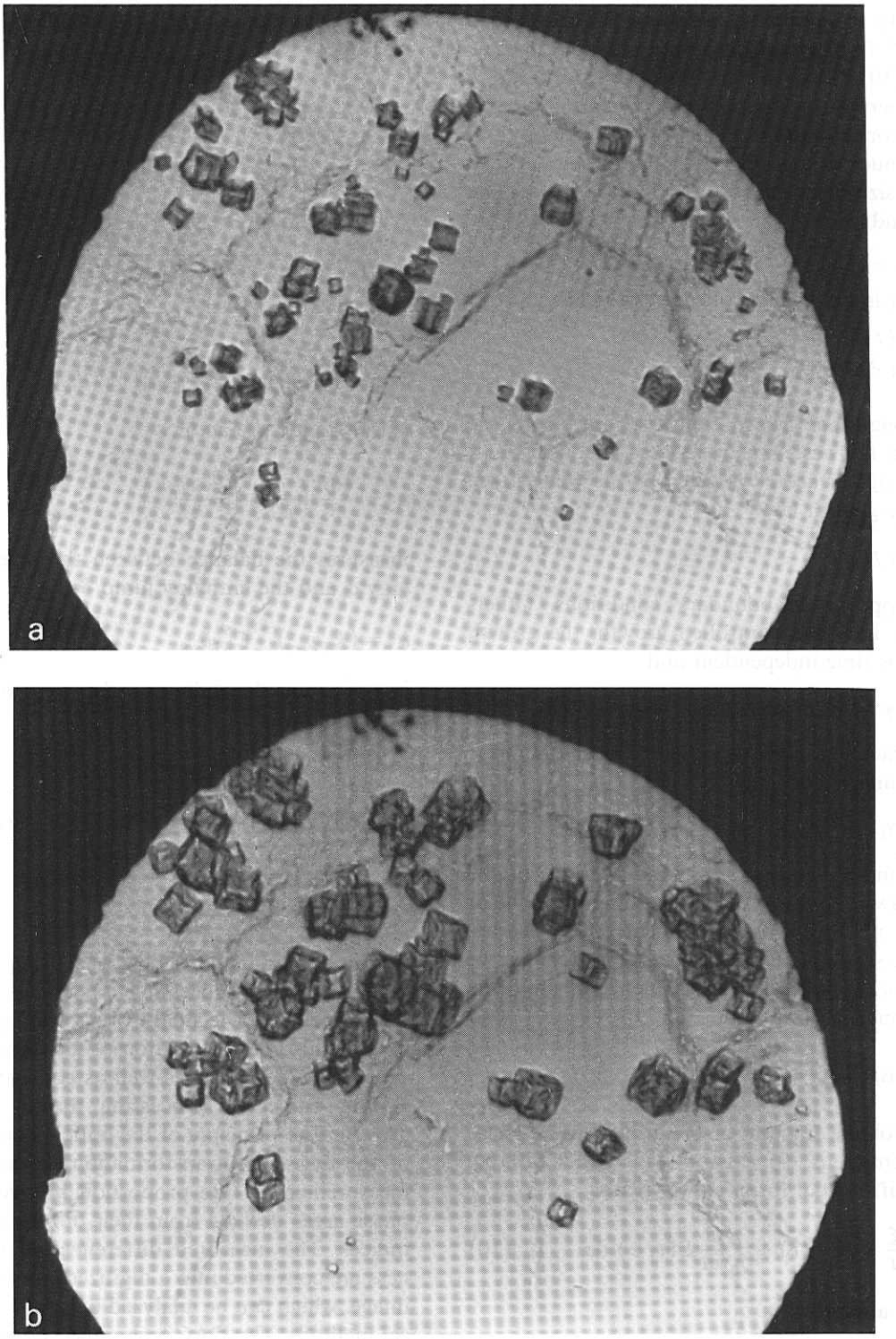

Fig. 2. Photograph of growing KCl crystals from supersaturated solution in the DAC. The time delay between the two snapshots (a) and (b) is 500 s. The diameter of the gasket hole is about 0.2 mm.

sure in solid-state investigations of micro-samples [12]. To achieve hydrostatic conditions, a metal-foil gasket with a small hole is interposed concentrically between the anvils. The hole is filled with the pressure-transmitting fluid, a 4 : 1 ethanol–methanol mixture with a certain amount of water. It also contains the sample under study, and one or more fragments of ruby which are needed for the pressure determination. In the kinetic experiments, a copper gasket is used which has a thickness of about 0.2 mm with a hole of about 0.2 mm diameter. The samples are polycrystalline potassium iodide and chloride in commercial quality (better than 99.9% purity), respectively. The determination of the degree of transformation is possible with a time resolution of 1 s. Moreover,

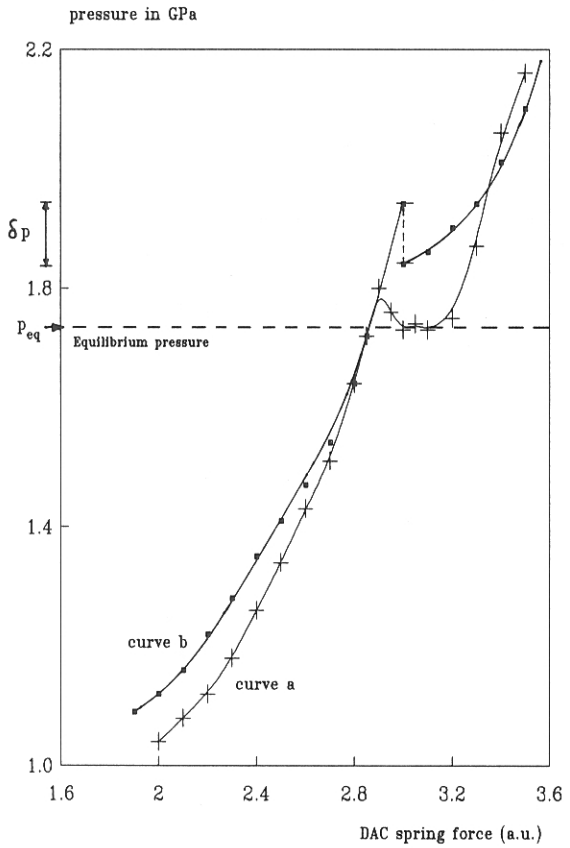

Fig. 3. Detected pressure (ruby scale) versus applied spring force on the DAC in the neighbourhood of the KI phase transition: (a) showing the equilibrium pressure relaxation; (b) yielding the maximum pressure depletion δp.

the image processing system supplies the possibility of a quantitative determination of various other kinetic parameters like nucleation rate or cluster-size distributions. As a consequence of our experimental setup, only a 2D projection of the transition process is detectable.

As experimentally observed, the low-pressure phase is to a great extent dissolved in the pressure-transmitting medium. This can be understood from the high solubility of the alkali halides in water [13]. The solubility of the crystals is additionally enhanced due to their very small grain size ($\lesssim 1$ μm), resulting from a first martensitic transformation process during the pre-compression of the filled gasket hole. The saturation concentration, however, is shifted down to extremely low values, as the applied pressure in the gasket hole reaches the stability range of the B2 modification. Therefore, we observe a nucleation and growth process of KI crystals (KCl crystals) with CsCl structure from a nearly homogeneous supersaturated solution. In an alternative preparation with a water-free pressure-transmitting fluid, no observations of growth processes from solution were found, but the B1 → B2 transition kinetics consists either of martensitic umklapp processes of small separated crystallites with domain structure or of recrystallization processes at preferred nucleation sites in the polycrystalline material. The existence of the B2 phase was independently verified by conventional angle-dispersive X-ray diffraction.

In the first stage of nucleation, the nuclei originate homogeneously distributed over the sample volume, indicating hydrostatic pressure conditions in the gasket hole. The crystals grow at small overpressures Δp in a stable faceted form, according to their cubic structure, with a slight tendency to the formation of skeletons known from alkali halides grown from aqueous solution [13], compare fig. 2. Passing through the intermediate stages of independent growth with practically zero nucleation rate and beginning competitive growth ("coarsening"), the crystal growth is slowly terminated in the final stage in consequence of the vanishing supersaturation $\Delta\mu \to 0$.

The pressure change during the phase transition in the sample volume of the DAC is indicated

by the relation between the applied spring force on the diamond anvils and the detected pressure values in the gasket hole (fig. 3, curve a). This can be used as a method for an accurate determination of the equilibrium pressure of both phases [14].

4. Results

4.1. Numerical solutions

For a quantitative examination, we solved the time scaled equation (10) (homogeneous nucleation rate in space, interface-controlled growth) numerically for some selected parameter sets a_2, a_3, a_4. In order to reduce the time consuming numerical procedure, the value of a_3 is estimated from the measured maximum pressure relaxation $\delta p = a_3 p_{eq}$ (fig. 3, curve b) to be equal to 0.0671. The two remaining parameters a_2 and a_4 therefore determine the transition characteristics.

At large Δp, the influence of the pressure depletion on the transition kinetics is negligible and the customary exponential transformation law holds. At low Δp, however, there are significant modifications. A typical example of the obtained solutions is shown in figs. 4 and 5 for $a_2 = 0.001$ and an overpressure of $a_4 = 0.06$. The most striking phenomena are the steep decrease of the nucleation rate at the beginning of the transition, the continouos decrease of the growth velocity, and, according to eq. (4), the saturation of the transformed volume fraction at 89.4% in the long time limit. These effects are again reflected by a nonlinear behaviour of the double-logarithmic plot $\ln(-\ln(1-\xi))$ versus $\ln(t)$ (see fig. 6).

The difference in the behaviour for large ($a_4 > a_3$) and low initial overpressures ($a_4 < a_3$) is seen from fig. 3, too: whereas in the former case the pressure relaxation leads to a discontinuous jump of its value at fixed external applied force (curve b), in the latter case the pressure remains in the neighbourhood of the equilibrium line with a transformed volume fraction less than 100% until the transition is completed (curve a).

The physical reason for the observed change in slope in fig. 6 is obviously the change of the supersaturation during the process. At the begin-

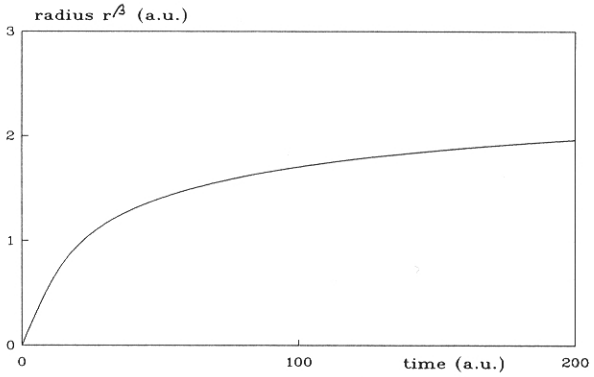

Fig. 5. Radius r^β of a growing spherical nucleus as a function of scaled time for the interface-controlled growth mechanism; parameters like fig. 4.

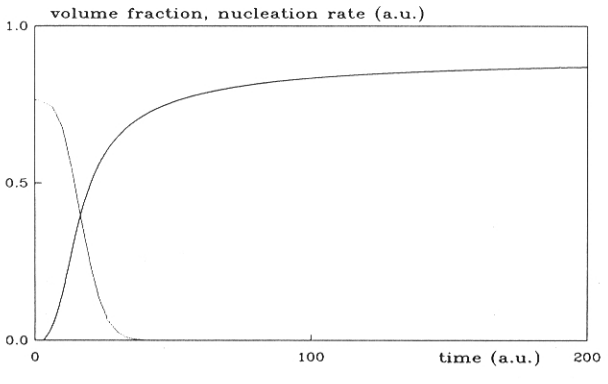

Fig. 4. Transformed volume fraction ξ and nucleation rate (broken line) in dependence of scaled time for $a_2 = 0.001$, $a_3 = 0.0671$, $a_4 = 0.06$ (numerical solution of eq. (10)).

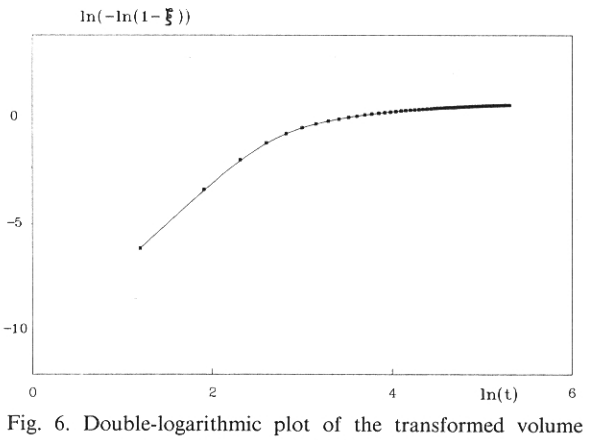

Fig. 6. Double-logarithmic plot of the transformed volume fraction $\xi(t)$ from fig. 4 ("Avrami plot").

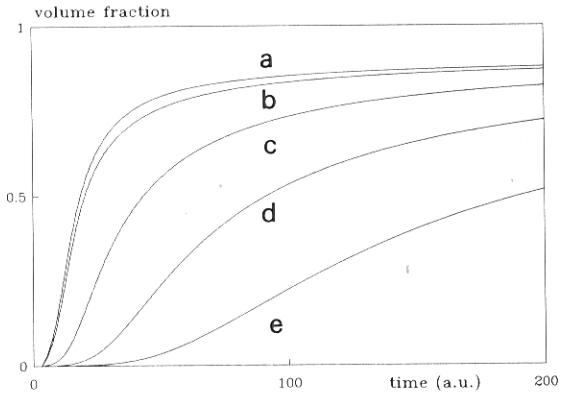

Fig. 7. Numerically calculated transformed volume fraction $\xi(t)$ for the interface-controlled growth mechanism with varying ratio a_2 of interfacial energy and enthalpy jump: (a) $a_2 = 0.0$; (b) $a_2 = 0 = 0001$; (c) $a_2 = 0.001$; (d) $a_2 = 0.01$; (e) $a_2 = 0.02$. For (a)–(e): $a_3 = 0.0671$ and $a_4 = 0.06$.

ning, the range of linear slope of the plot is a consequence of the Avrami-like behaviour of a nearly infinite system with constant nucleation and growth rates ("Avrami exponent"). When ξ exceeds a value of about 10%, the pressure depletion firstly suppresses any possible nucleation events, and secondly leads to a gradual reduction of the growth rate. For very long times, the transformation terminates in the steady state with $\xi = a_4/a_3$ (if $a_4 < a_3$).

The influence of the a_2 parameter is illustrated in fig. 7. With given overpressure a_4, the same saturation value of ξ is reached in either relative short times (a_2 very small) or with a significant delay time ($a_2 \gtrsim 0.001$). This is caused by the strong dependence of the nucleation rate on the surface tension, which may considerable stunt the transition kinetics. In the double-logarithmic plot of fig. 8, the above discussed change in slope is again observable. An increasing order of magnitude of surface tension is here reflected by an extension of the linear slope region to larger times.

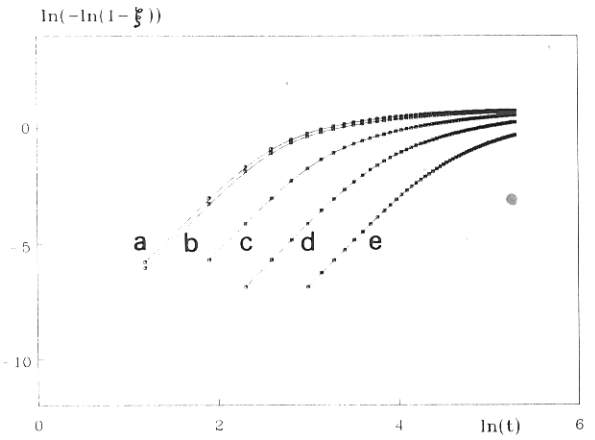

Fig. 8. Double-logarithmic plot of the transformed volume fractions of fig. 7.

4.2. Comparison with the experimental data

A typical set of the measured transformation curves showing the growth of the crystalline B2 phase from solution is depicted in fig. 9, together with the corresponding Avrami plots in fig. 10. It reveals the same qualitative features as discussed above. The saturation behaviour below 100% and the nonlinear bending of the double-logarithmic plot are obviously confirmed by the experimental results. In order to allow for a quantitative comparison, a two-dimensional projection of the

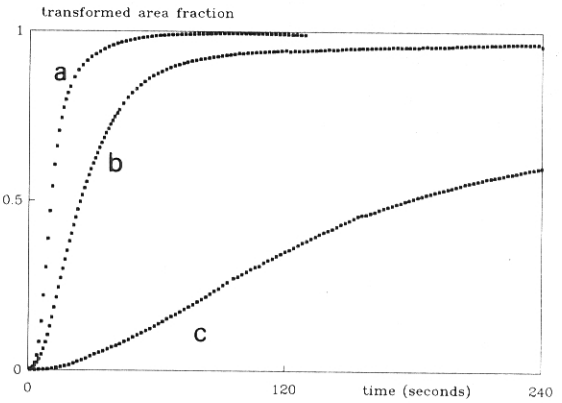

Fig. 9. Measured transformed area fraction ξ^{2D} of growing B2 crystals from solution in the DAC versus time (using the image processing system with a time resolution of 1 s) for different initial overpressures, the sample is polycrystalline potassium iodide with $p_{eq} = 1.75$ GPa: (a) $p(t = 0) = 1.87$ GPa; (b) $p(t = 0) = 1.84$ GPa; (c) $p(t = 0) = 1.78$ GPa; The precise value of the determined equilibrium pressure p_{eq} is dependent on the water fraction in the pressure-transmitting medium, which is in our experiments in the order of or less than 5%.

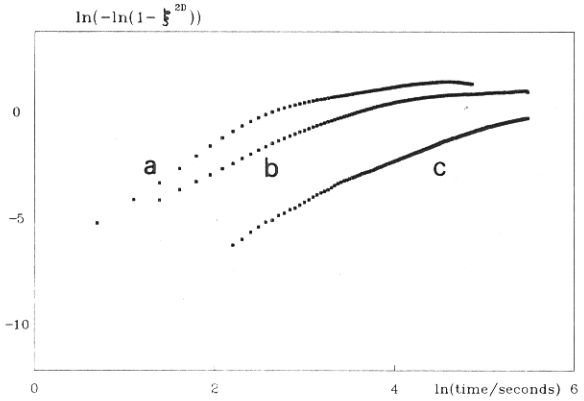

Fig. 10. Double-logarithmic plot of the transformed area fractions of fig. 9.

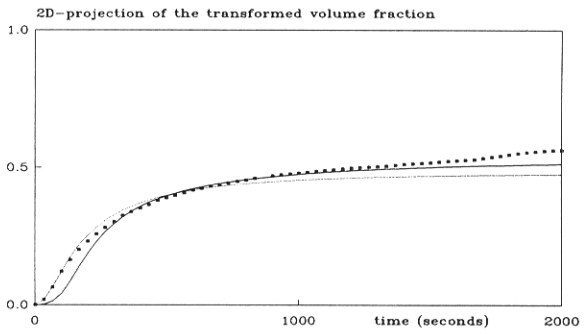

Fig. 11. Comparison between the measured transformed area fraction ξ^{2D} in potassium chloride and the numerical solution of the modified Avrami equation with given maximum pressure depletion $a_3 = 0.0671$ and initial overpressure $a_4 = 0.02$ for two different growth mechanisms. The fitting parameters are a_1 and $a_2 = 0.0012$. (· · · · · ·) Diffusion controlled; (———) interface controlled; (■) experimental data.

volume transformation rate $\xi(t)$ is needed. This can be done utilizing the relation

$$\xi^{2D}(t) = 1 - \exp\left[- \int_0^t I^A(s)\, v_s^{2D}(t)\, \mathrm{d}s \right], \qquad (11)$$

where $I^A(s)$ is the nucleation rate per unit area and $v_s^{2D}(t)$ is the 2D projection of a growing nucleus. Both functions must be calculated on the basis of the real 3D-transformed volume fraction ξ. If the adjusted focus depth of the microscope is sufficient small, the detected rate $I^A(s)$ is equal to $I^V(s)$ up to an unimportant constant factor (which only shifts the used time scale a_1). Therefore, the essential correction in eq. (11) is due to $v_s^{2D}(t)$. The numerical integration with some selected parameter sets show two main effects of the 2D projection:

(a) a shift of the time scale of the transformation;
(b) the enhancement of the asymptotically reached transformed area fraction ξ^{2D} compared with $\xi(t \to \infty)$.

A further but expected consequence of the 2D projection is the diminishing of the slope of the initial linear range ("Avrami exponent") of $\ln(-\ln(1-\xi))$ by unity (e.g. for time-constant nucleation and growth rates its value is diminished from 4 to 3).

Because of the uncertainty of a_1 and a_2, these parameters are used to fit the experimental data. The result of such a procedure for a given initial overpressure of $a_4 = 0.02$ is shown in fig. 11. It can be seen, that the beginning transformation stages show a rather diffusion controlled growth rate, contrary to the tendency to an interface controlled growth rate at later stages. This at the first instance surprising result is confirmed by inspection of fig. 2: At the beginning small crystals grow faster than larger ones. Therefore, we have to state a kind of cross-over behaviour in the growth mechanism during the transition process. At larger stages, the slight deviation of the experimental results from the modified Avrami model could result from possible impacts of the growing crystals

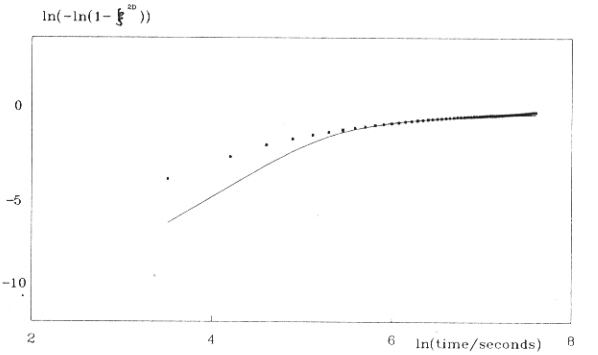

Fig. 12. Double-logarithmic plot of the transformed area fraction of fig. 11. (· · · · · ·) Diffusion controlled; (———) interface controlled; (■) experimental data.

on the diamond anvils, which are not included in the present theory.

A further interesting consequence is obtained for the growth of a fixed isolated nucleus. Though the interface-controlled growth rate is time-independent, it follows a nonlinear characteristics in the plot of the growing radius versus time (fig. 5). One should therefore take care in determining growth velocities or other kinetic quantities in the DAC [15].

5. Discussion

The optical observation method has, despite their facilities for differential image processing and for high time resolution measurements, two specific problems. First, at the beginning stages of the transition nucleus dimensions less than ~ 1 μm cannot be detected. The experimentally obtained transformed volume fractions in that range have therefore a relative large uncertainty. Second, a volume projection into a two-dimensional plane instead of the volume transformation is measured. If one looks for other kinetic data such as grain size distributions or the development of correlation functions, eq. (11) of course must replaced by a more elaborated theory.

The problem of a two-dimensional cut through the microstructure of grains resulting from a three-dimensional nucleation and growth process is of special theoretical interest in the literature, but only few rigorous results are up to now known in the limit $\xi = 1$ [16]. Here, for our purposes, our determination of the degree of transformation is sufficient, which is much easier realized by the described method.

A consequence of the limited spatial resolution is that the real nucleation process cannot be detected. This corresponds formally with a virtual critical nucleus size in the order of 1 μm. On the other hand clustering of different crystals below this threshold value would lead to an observable contribution to the detected new phase fraction and would therefore disagree with such a formal model description. More recently, Srolovitz and coworkers [17] have determined the influence of the finite critical nucleus size on the double-logarithmic plot by a numerical simulation technique. It would be interesting whether the inclusion of this effect in eq. (10) leads to similar results in the frame of the Avrami model.

The above mentioned problems can be avoided using a standard energy-dispersive X-ray diffraction system combined with the DAC, compare, e.g., ref. [18]. Actually. the authors have found a nonlinear bending of the double-logarithmic plot too, but they explained this effect in terms of a site saturated nucleation and growth regime originally proposed by Cahn [19]. In our experiments with growth from the solution, such an explanation is not reasonable. Moreover, we believe that our proposed mechanism is quite general true for any first-order phase transitions in the DAC in hydrostatic preparation with a significant volume jump between both phases.

6. Conclusion

We have demonstrated that nucleation and growth processes under isochoric constraints show significant deviations from the well-known Avrami behaviour:

(1) a steep decrease of the nucleation rate immediately after the beginning stages;

(2) a gradual diminishing growth rate during the transformation process;

(3) the termination of the transition before the volume fraction of the new phase reaches 100%.

Beside their general interest such processes may play an important role in special petrographic problems such as crystallization in small rock inclusions. More recently, Andreazza and coworkers [20] have stressed the applicability of nucleation models in confined space to the crystallization in gels. In any case, the diamond anvil cell is a convenient and useful tool for the experimentalist to check these model conceptions.

Acknowledgements

The authors wish to thank A. Kraft, M. Ziemann, R. Gratz and B. Lorenz for their helpful discussions.

References

[1] For a general review, see: J.W. Christian, The Theory of Phase Transformations in Metals and Alloys, Part I (Pergamon, Oxford, 1975).
[2] W.A. Johnson and R.F. Mehl, Trans. Am. Inst. Min. Engrs. 135 (1939) 1103.
[3] M. Avrami, J. Chem. Phys. 7 (1939) 1103.
[4] M. Avrami. J. Chem. Phys. 8 (1940) 212.
[5] M. Avrami, J. Chem. Phys. 9 (1941) 177.
[6] A.E. Kolmogorov, Izv. Akad. Nauk SSSR, Ser. Mat. 1 (1937) 355.
[7] H. Haken, Synergetik (Springer, Berlin, 1983).
[8] W. Ebeling and H. Ulbricht, Eds., Selforganization by Nonlinear Irreversible Processes, Springer Series in Synergetics, Vol. 33 (Springer, Berlin, 1986).
[9] H. Ulbricht, J. Schmelzer, R. Mahnke and F. Schweitzer, Thermodynamics of Finite Systems and the Kinetics of First-Order Phase Transitions (Teubner, Leipzig, 1988).
[10] J. Schmelzer, Z. Physik. Chem. 266 (1985) 1057.
[11] R. Dässler, High Temp.-High Pressures 21 (1988) 661.
[12] A. Jayaraman, Rev. Mod. Phys. 55 (1983) 65.
[13] I. Tarjan and M. Matrai, Eds., Laboratory Manual on Crystal Growth (Akademiai Kiado, Budapest, 1972).
[14] M. Riedel and R. Dässler, presented at 12th AIRAPT Conf. on High Pressure Science and Technology, Paderborn, 1989.
[15] T. Sawada, K. Takemura, K. Kitamura and S. Kimura, J. Crystal Growth 88 (1988) 535.
[16] K.W. Mahin, K. Hanson and J.W. Morris, Jr., Acta Met. 28 (1980) 443.
[17] D.J. Srolovitz, G.S. Grest, M.P. Anderson and A.D. Rollett, Acta Met. 36 (1988) 2115.
[18] N. Hamaya and S. Akimoto, High Temp.-High Pressures 13 (1981) 347.
[19] J.W. Cahn, Acta Met. 4 (1956) 449.
[20] P. Andreazza, F. Lefaucheux and B. Mutaftschiev, J. Crystal Growth 92 (1988) 415.